# Molecular Complexes of Superoxide Ion with Maleic Anhydride and Its Analogues

**Yoshio Nosaka,* Akira Kira, and Masashi Imamura**

*Contribution from the Institute of Physical and Chemical Research, Wako-Shi, Saitama 351, Japan.* *Received August 15, 1979*

**Abstract:** Oxygenated 2-methyltetrahydrofuran glasses containing maleic anhydride (MA) were $\gamma$-irradiated at 77 K followed by warming, and optical and ESR spectra were measured. Two species peculiar to the presence of both MA and $O_2$ were found: one that appears at earlier stages is characterizied by both a broad optical absorption band at 432 nm and an ESR band with $g_z = 2.047$, and the other that follows this possesses an optical band at 640 nm and an ESR band with $g_z = 2.055$. The features of the observed ESR spectra including those for $^{17}O_2$ indicate that these species are most likely molecular complexes, $O_2^- \cdots$ MA and $O_2^- \cdots (MA)_2$, respectively. Similar optical and ESR spectra were also observed for methyl- and dimethylmaleic anhydride, maleimide, and fumaronitrile.

## Introduction

The superoxide ion $O_2^-$ draws attention because of its specific reactivities to living tissues, and its chemical reactivities have been extensively studied. The superoxide ion is prepared in the laboratory by radiolysis,[1,2] UV photolysis,[3] electrolysis,[4] and also dissociation of $KO_2$[5] or $NaO_2$.[6] The superoxide ion is also formed on the surfaces of certain catalytic solids.[7]

This paper describes the observation of molecular complexes which contain oxygen in the form of $O_2^-$. The complexes were observed in 2-methyltetrahydrofuran (MTHF) glassy solutions containing both oxygen and maleic anhydride (MA) or its analogues—methylmaleic anhydride, dimethylmaleic anhydride, maleimide, and fumaronitrile—on irradiation at 77 K followed by carefully controlled annealing. Observation was also made by pulse radiolysis at 115 K. Environmental interactions are necessary for the ESR spectrum of $O_2^-$ to be detected,[2] and in that sense the superoxide ions so far observed interact more or less with a solvent, surface, or counterion. In the complex found in this study, it is a specific solute molecule that interacts with $O_2^-$. As far as we are aware, this is the first observation of a molecular complex in which $O_2^-$ is involved.

Radiation-chemical processes which closely relate to the present experiments are summarized as follows. $\gamma$-Irradiation of MTHF glasses containing a solute results in the selective formation of solute anions without the formation of solute cations;[8] therefore, the probable species occurring in the irradiated glasses are solute anions, residual trapped electrons, protonated MTHF, and neutral radicals originating in MTHF. It should be noted that the protonated MTHF, as a hydronium ion in water, gives no absorption signals in either ESR or usual optical spectroscopy. In the present experiments, solute concentrations were so high that trapped electrons were all converted to solute anions. Subsequent warming or annealing enables the radiation-induced species and solute molecules to diffuse and react with one another. Warming-induced reactions such as associated dimer-ion formation occur effectively before ions are removed by charge recombination.[9,10]

## Experimental Section

Both optical-absorption and ESR spectra were taken at 77 K first after $\gamma$-irradiation at 77 K at a dose rate of $3.4 \times 10^{21}$ eV kg$^{-1}$ min$^{-1}$ and then occasionally in the course of subsequent warming. A JEOL FE-3AX ESR spectromter at X band and a Cary 14 RI spectrophotometer were used. The magnetic field was calibrated with the splitting of $Mn^{2+}$ and $g$ values were calculated by using $g = 2.0026$ for $TCNQ^-$ crystals. A pulse radiolysis apparatus used for kinetic measurement has been described elsewhere.[9] In this study, 1-$\mu$s pulses with a peak current of ca. 120 mA were delivered from a Van de Graaf accelerator operating at 2.5 MV. Samples were saturated with oxygen at ca. 1 atm at room temperature immediately before irradiation, unless otherwise stated.

Wako Junyaku's MTHF was fractionally distilled and then stored over sodium–potassium alloy in a degassed vessel until preparation of samples. Maleic anhydride and fumaronitrile were recrystallized from ether and from a mixture of THF and petroleum ether, respectively. Other chemicals for solutes were used as supplied. The oxygen gas containing 25% $^{17}O$ was purchased from CEA, France.

## Results

The optical absorption spectra in an oxygenated MTHF glass containing MA are shown in Figure 1. The spectrum immediately after irradiation consists of a near-UV band which has been assigned to maleic anhydride anions $MA^-$ [9,11] and a tailing band below ca. 2.4 $\mu m^{-1}$ induced by oxygenation. The tailing band did not emerge in the absence of $O_2$. On warming, a band with a maximum at 432 nm arises first, accompanied by disappearance of the $MA^-$ band. The 432-nm band is replaced by a band with a peak at 640 nm on further warming. The tailing band in the initial spectrum seems due to the 432- and 640-nm bands, which probably appear to a small extent even before warming. The presence of both MA and oxygen was essential to the appearance of 432- and 640-nm bands. When the oxygen concentration was reduced, maximum yields of both 432- and 640-nm bands during warming decreased and a spectrum of dimer anions $(MA)_2^-$ [9] appeared in the IR region. In the absence of oxygen, only the $(MA)_2^-$ spectrum is observed, as has been reported by Arai et al.[9]

The same processes observed in warmed glasses were traced using the pulse radiolysis method. The oxygen concentration was reduced, though not determined exactly, in order to visualize the competition between dimer-anion formation and 432- and 640-nm band formation. Temperature was raised to 115 K, where the reactions of concern proceed at adequate rates. Figures 2 and 3 show the change in the transmittance with time at characteristic wavelengths: 360 nm for $MA^-$ and 1000 nm for $(MA)_2^-$ as well as 435 and 625 nm for the oxygen-induced species. The traces for 1000 nm, where only $(MA)_2^-$ absorbs,[9] indicate that the concentration of MA for Figure 2 (0.05 M) is small enough to avoid $(MA)_2^-$ formation

$$MA^- + MA \rightarrow (MA)_2^- \quad (1)$$

but that for Figure 3 (0.5 M) is large enough to allow this reaction. In Figure 2 the growth of the 435-nm absorption coincides with the decay of the $MA^-$ band at 360 nm, and the decay of the 435-nm absorption seems to correspond to the growth at 625 nm. These findings are consistent with the expressions

$$MA^- + O_2 \rightarrow (O_2 \cdots MA)^- \quad (2)$$

$$(O_2 \cdots MA)^- + MA \rightarrow (O_2 \cdots (MA)_2)^- \quad (3)$$

0002-7863/80/1502-1949$01.00/0 

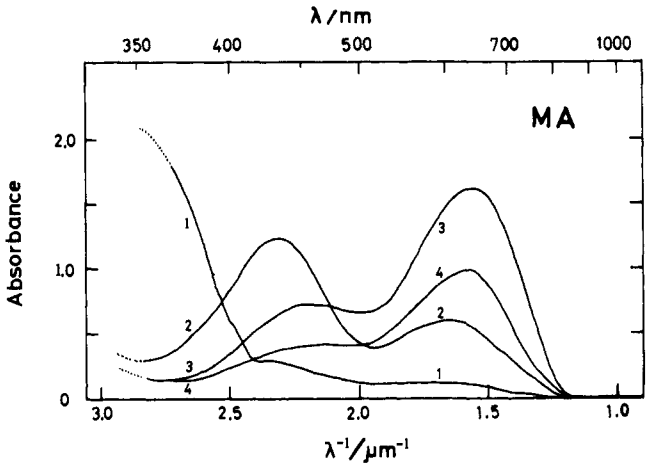


**Figure 1.** Absorption spectra for maleic anhydride (0.5 M) in oxygenated MTHF glassy solution after γ-irradiation to a dose of $1.7 \times 10^{22}$ eV kg$^{-1}$: before warming (curve 1) and after warming at 98 K for 15 s (curve 2), 2 min (curve 3), and 3 min (curve 4), measured at 77 K. The sample was irradiated in a Spectrosil tube of 4-mm diameter.

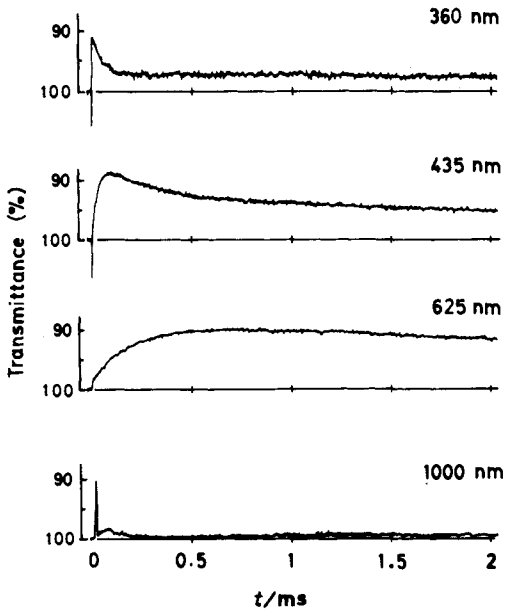


**Figure 2.** Growth and decay of absorption in an oxygenated MTHF solution of 0.05 M maleic anhydride at 115 K after electron pulse irradiation.

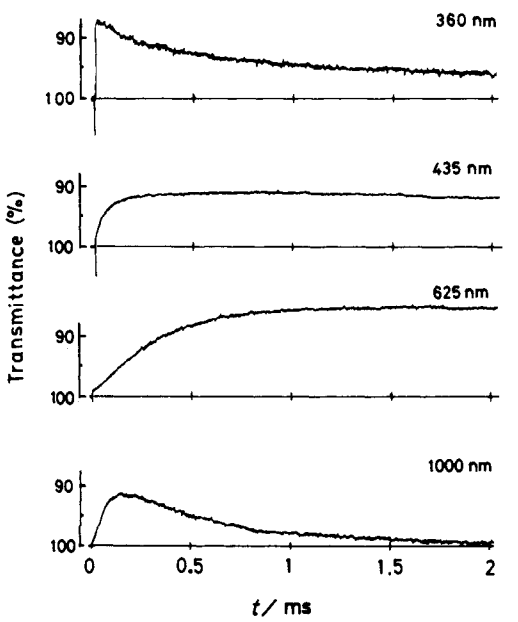


**Figure 3.** Growth and decay of absorption in an oxygenated MTHF solution of 0.5 M maleic anhydride at 115 K after electron pulse irradiation.

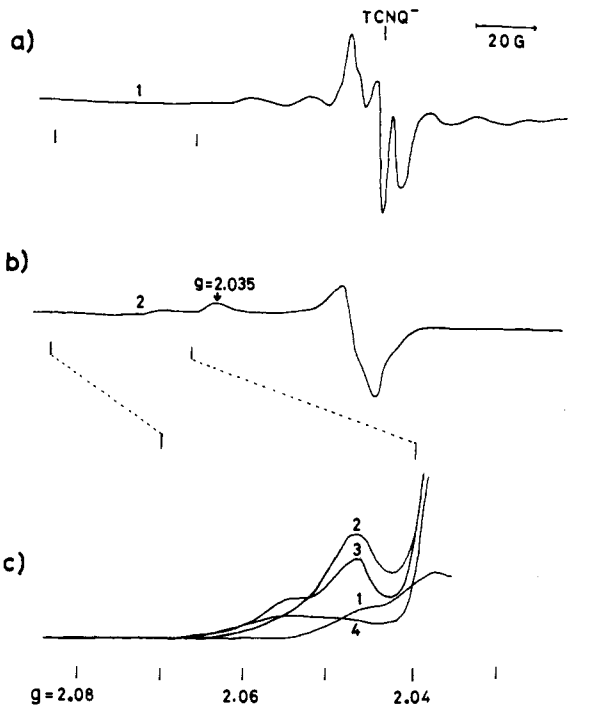


**Figure 4.** ESR spectra for the same sample as in Figure 1. Numbers correspond to those in Figure 1. (a) Immediately after γ-irradiation; (b) after warming at 98 K for 15 s; (c) expanded spectra of (a) and (b) and those after further warming. The gain is the same for (a) and (b) and ×20 for (c).

where the 432- and 640-nm bands are tentatively assigned to complex anions containing MA and $(MA)_2$, respectively. A complete interpretation of Figure 3 is difficult because of overlap of dominant absorptions of other species at 435 and 360 nm. However, it can be concluded from Figure 3 that the 625-nm absorption grows concurrently with the decay of $(MA)_2^-$. This can be represented as

$$(MA)_2^- + O_2 \rightarrow (O_2 \cdot \cdot \cdot (MA)_2)^- \qquad (4)$$

Formation of the complex anions, tentatively assumed above, is concluded from the results of ESR measurements which will be described below.

Figure 4 exhibits the ESR spectra, taken at the same warming steps, of the same samples used for measurement of the optical spectra in Figure 1. The initial ESR spectrum shown in (a) almost agrees with the spectrum observed previously in a deaerated MTHF glass containing MA,[12] which consists of seven broad lines of MTHF radicals with large hyperfine splitting and four lines of $MA^-$. On warming, spectrum (a) was replaced by the spectrum shown in (b). The main species of this spectrum has an orthorhombic $g$ tensor with $g_z = 2.035$. The signals in the high $g$ region are expanded in (c), where other signals for further warming are also depicted. Two separate lines with $g$ values of 2.047 and 2.055 also appeared during warming. In the absence of MA, the line at 2.035 was observed but the other two were not. Previous studies have revealed that peroxide radicals are usually characterized by a line with $g_z$ value close to 2.033.[2] Consequently, the line at 2.035 in Figure 4b can be assigned to an MTHF peroxide

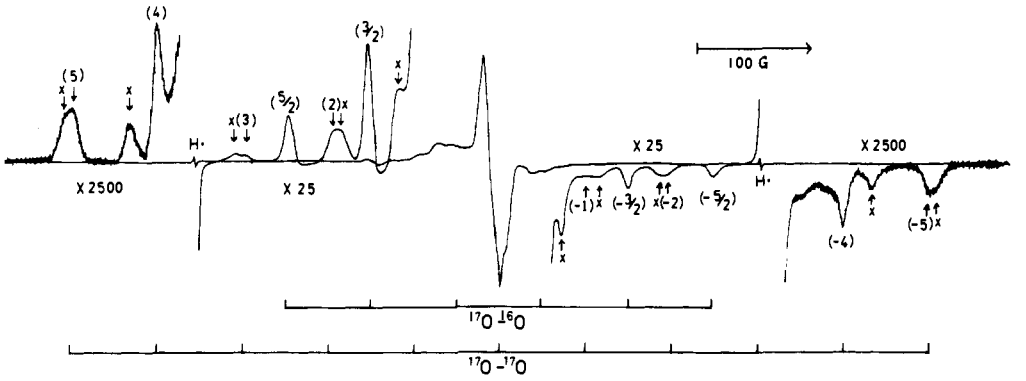


**Figure 5.** ESR spectrum of a MTHF glass containing both maleic anhydride (0.5 M) and 25% $^{17}O$-enriched oxygen irradiated to a dose of $1.0 \times 10^{23}$ eV kg$^{-1}$. The sample was annealed at 98 K for 15 s before measurement at 77 K. Numbers in parentheses are total nuclear spin quantum number ($M_I$) of $O_2$. Signals indicated by X are those observed in the absence of maleic anhydride.

radical. The large central signal in Figure 4b is considered to consist of lines corresponding to $g_x$ and $g_y$ for the peroxide radical and other warming-induced species. No attempts to isolate each line were made.

The ESR signal with $g_z$ of 2.047 evolves concomitantly with that of the 432-nm optical band, and the signal with $g_z$ of 2.055 corresponds to the 640-nm band, as seen from comparison of Figure 4c with Figure 1. Thus, these ESR signals are due to the complex anions to which the 432- and 640-nm bands are assigned. The values for $g_z$ of $O_2^-$ are higher than $g_z$ of peroxide radicals;[2] therefore, $g_z$ values of 2.047 and 2.055 are most likely assigned to those of $O_2^-$. It is known that ESR signals of $O_2^-$ are detectable only under environmental perturbations[2] and that ethers are too weak as a medium to cause such a perturbation. In fact, no signals of $O_2^-$ were observed in oxygenated MTHF without MA, though the trapped-electron yield was reduced by oxygenation probably because of $O_2^-$ formation. Is is also known from pulse radiolysis studies that dissolved $O_2$ captures electrons in aprotic solvents.[13] Thus, MA or a species originating in MA is considered to be responsible for a perturbation to visualize the ESR signal of $O_2^-$ in the present system; in other words, such complex anions as shown in reactions 2-4 are formed. Furthermore, the lack of fine structure for $MA^-$ in the main part of the ESR signal in Figure 4b indicates that the perturbing species, MA, does not contain appreciable free spin; accordingly, free spin in the complex anions is mainly localized on an oxygen molecule.

Further information on spin distribution in the complex anions was obtained by the use of $^{17}O_2$. The nuclear spin of $^{17}O$ is $5/2$. Figure 5 shows the ESR spectrum observed after annealing in a sample saturated with 25% $^{17}O$-enriched oxygen. Positions of lines of the MTHF peroxide radical containing $^{17}O$, measured in a glass without MA, are marked by X. The other part of the spectrum is explicable in terms of six lines due to hyperfine splitting by $^{17}O$ of $^{17}O\text{-}^{16}O$ with $M_I$ values of half-integer and 11 lines due to $^{17}O\text{-}^{17}O$ with $M_I$ values of integer, as illustrated in Figure 5. The hyperfine coupling constant was 75 G for both splittings. When the electron spin is equally distributed over two oxygen atoms, the intensities of lines split by $^{17}O\text{-}^{17}O$ are expected to be in ratios of 1:2:3:4:5:6:5:4:3:2:1. The observed intensities of the lines for $M_I$ values of $\pm 1$ to $\pm 5$ support these ratios qualitatively, though the central part of the signal is concealed by a predominant signal of the peroxide radical. The equal spin distribution on two oxygen atoms suggests that both the atoms equally interact with MA or $(MA)_2$ in the complex anions.[14]

The observed hyperfine splittings of $^{17}O$ are associated with $g_x$ or $g_y$; no splittings for the signal of $g_z$ were detected. Che and co-workers have measured the hyperfine splitting constant of $^{17}O$ for $O_2^-$ adsorbed on oxides such as MgO[15] and Mo/$SiO_2$,[14] which is close to our value. They assigned the observed splitting to $A_x$ and estimated that $A_y = A_z = 0$. Consequently, our failure to detect $A_z$ splittings may be attributed to the smallness of the $A_z$ value. If $A_y$ and $A_z$ for $O_2^-$ are also nil in the present case, spin densities in s and p orbitals are calculated to be 1.5 and 48.5%, respectively, using values of 1655 and 51.5 G for $A_0$ and $B_0$, respectively.[16] Thus, 100% of the unpaired electrons are located on $O_2^-$ in the complex anions and most of them occupy p orbitals. No difference in the value for $A_x$ was detectable between the two complex anions.

**Table I.** Optical-Band Energies and ESR Parameters for $O_2^-$ Complexes

| compd | $\lambda_{max}$, eV | $g_z$ | $\epsilon_1\epsilon_2/(\epsilon_2 - \epsilon_1)$, eV[a] | $A_x$, G |
|---|---|---|---|---|
| maleic anhydride | 2.87 | 2.047 | 0.62 | 75 |
| (MA) | 1.94 | 2.055 | 0.53 | |
| methylmaleic anhydride | 2.91 | 2.054 | 0.54 | 75 |
| (MMA) | 2.05 | 2.06 | 0.5 | |
| dimethylmaleic anhydride | 2.95 | 2.060 | 0.48 | 75 |
| (DMMA) | 2.10 | 2.073 | 0.35 | |
| fumaronitrile (FN) | 3.01 | 2.058 | 0.50 | 76 |
| | 2.25 | 2.114 | 0.25 | 74 |
| maleimide (MI) | 2.79 | 2.060 | 0.48 | 75 |
| | 2.21 | 2.07 | 0.4 | |

[a] Calculated from $g_z$ using eq 11 with $\zeta = 0.014$ eV.[17]

The above analysis of the ESR spectra leads to the conclusion that the complex anions are eventually in the forms of $O_2^-\cdots MA$ and $O_2^-\cdots(MA)_2$. In the present experiments, the complex anions were produced via $MA^-$ and $(MA)_2^-$, because high MA concentrations favored their observation under the condition of saturation with 1 atm of oxygen. Other possible reactions such as

$$O_2^- + MA \rightarrow O_2^-\cdots MA \qquad (5)$$

which might predominate at higher oxygen concentrations were not confirmed positively.

Measurement was also carried out for analogous solutes: methylmaleic anhydride (MMA), dimethylmaleic anhydride (DMMA), fumaronitrile (FN), and maleimide (MI). The results were essentially similar to those for MA as follows, and can be interpreted in the same manner. The optical absorption spectra are shown in Figure 6. Vibrational structures seen in the monomer-anion bands in the near UV region of MMA, DMMA, and FN disappear in the warming-induced bands. The lack of structure in the latter bands suggests that the latter do not result from the shift of the former. The ESR spectra in the region near $g_z$ of $O_2^-$ are shown in Figure 7. Two different ESR lines for each compound correspond to the two optical bands, as in the case of MA. Two $g_z$ values and corresponding optical-band energies at $\lambda_{max}$ are listed in Table I. Hyper-

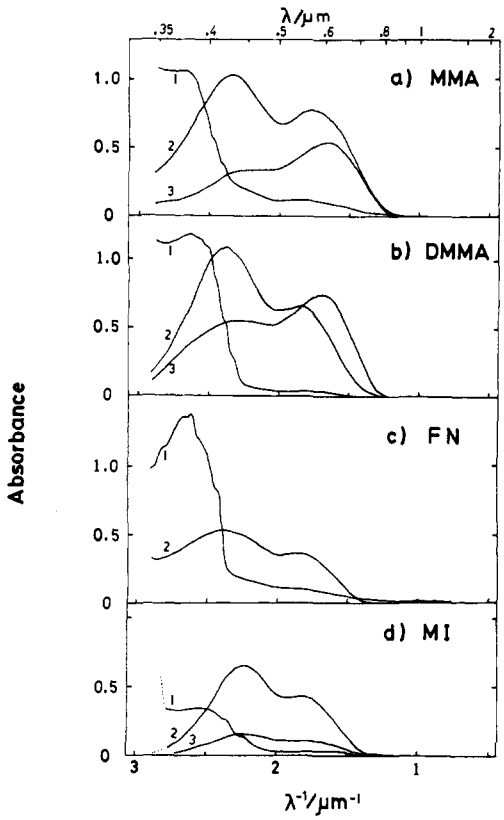


**Figure 6.** Absorption spectra measured at 77 K after γ-irradiation of oxygenated MTHF solutions in a cell 1.5 mm in thickness. Curve 1 is the spectrum after the irradiation to a dose of $3.4 \times 10^{22}$ eV kg$^{-1}$, and curves 2 and 3 are after subsequent warming.

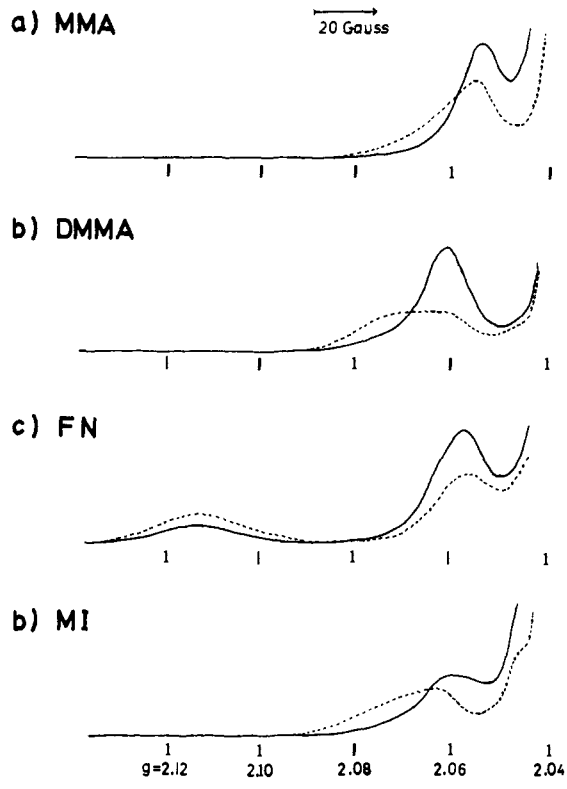


**Figure 7.** Low-field part of ESR spectra in oxygenated MTHF glassy solutions on γ-irradiation followed by warming (measured at 77 K). Warming periods at 98 K are (a) 10 and 60, (b) 20 and 110, (c) 20 and 50, and (d) 0 and 10 s for solid and dotted lines, respectively, which gave good separation of two lines in each solution.

fine-coupling constants of $^{17}O$ measured for these compounds are also listed in Table I. No appreciable difference in $A_x$ was found between two complex anions except for the case of FN.

## Discussion

The intermolecular interaction probably takes place between one of the degenerate SOMO (singly occupied molecular orbitals) of $O_2$ and SOMO of electron-donor anions $M^-$. If we take the geometry of the complex as shown in Figure 8, the interacting orbitals are denoted by $\pi_y^*$ and $\pi_M^*$. The other SOMO of $O_2$, $\pi_x^*$, is hardly affected by $\pi_M^*$ because of symmetry. This theoretical expectation is compatible with the finding that the hyperfine splitting constant $A_x$ remains almost unchanged for various donors as shown in Table I.

The amount of the energy-level splitting between degenerate $\pi^*$ orbitals of $O_2$ has been discussed with relation to the $g_z$ value of the ESR spectrum for $O_2^-$.[15,17] The principal value of an orthorhombic $g$ tensor for a principal axis $x$ is theoretically expressed by the equation[18]

$$g_x = 2.0023 + 2\sum_n \sum_{k,j} \frac{\langle 0|\zeta_k L_{xk}|n\rangle \langle n|L_{xj}|0\rangle}{E_0 - E_n} \qquad (6)$$

Here the summation is over all pairs of atoms $k$ and $j$, $L_{xk}$ represents the angular-momentum operator for the atomic orbitals of $k$, $\zeta_k$ denotes a spin-orbit coupling constant of atom $k$, $|0\rangle$ and $|n\rangle$ are wave functions of SOMO for ground and excited states, respectively, and $E_0$ and $E_n$ are energies of these orbitals. This equation indicates that higher excited states should contribute less to the $g$ values. In the present case, the SOMO of the ground state is $(\pi_x^*)'$, and two molecular orbitals $(\pi_y^*)'$ and $(\pi_M^*)'$ are considered to contribute mainly to eq 6 as SOMO of excited states. These three orbitals are expressed by

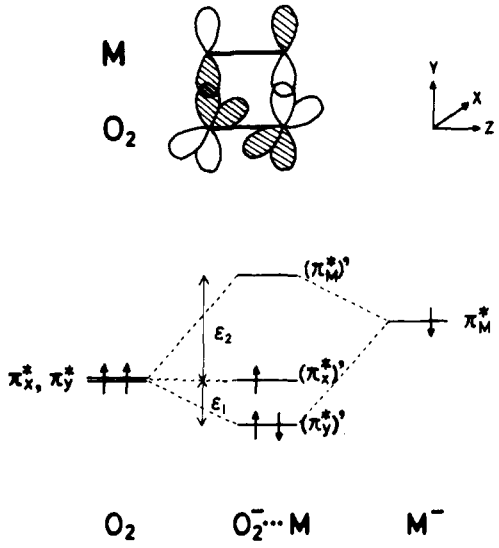


**Figure 8.** Energy-level diagram for the interorbital interaction between the ethylene group of anion $M^-$ and molecular oxygen $O_2$.

$$(\pi_x^*)' = \pi_x^*$$

$$(\pi_y^*)' = C_1\pi_y^* + C_2\pi_M^* \qquad (7)$$

$$(\pi_M^*)' = C_2\pi_y^* - C_1\pi_M^* \qquad (8)$$

where the coefficients $C_1$ and $C_2$ are approximately given by

$$C_1^2 = \epsilon_2/(\epsilon_1 + \epsilon_2) \qquad C_2^2 = \epsilon_1/(\epsilon_1 + \epsilon_2) \qquad (9)$$

Thus, eq 6 is simplified as

$$g_x \simeq g_y \simeq 2.0023 \qquad (10)$$

$$g_z \simeq 2.0023 + 2\zeta\frac{\epsilon_2 - \epsilon_1}{\epsilon_1\epsilon_2} \quad (11)$$

The values of $\epsilon_1\epsilon_2/(\epsilon_2 - \epsilon_1)$ listed in Table I were calculated from the observed $g_z$ values using eq 11 with a $\zeta$ value of 0.014 eV given by Kasai.[17]

The positive values of $\epsilon_1\epsilon_2/(\epsilon_2 - \epsilon_1)$ suggest that the SOMO of $M^-$, $\pi_M$*, lies above the SOMO of $O_2^-$, $\pi_x$*. The energy level of SOMO for radical anions usually relates to the electron affinity of the parent molecule.[19] The observed $g_z$ values require that in MTHF glass the electron affinity of $O_2$ should be higher than that of any solute compounds used. Although the experimental values for the electron affinity (EA) are not accurate,[20] the values of 1.74 ($O_2$),[4] 1.64 (MA),[21] 1.13 (FN),[22] and 1.80 (MI)[23] eV, based on the equation[20]

$$\mathrm{EA} = E_{1/2} + 2.49 \pm 0.26 \quad (12)$$

where $E_{1/2}$ is a half-wave reduction potential, can be regarded as rather consistent with the above requirement. Although the electron affinity of $O_2$ estimated above is much larger than that in the gas phase (0.44 eV),[24] there is evidence supporting such a high value in condensed phases: Sowada and Holroyd[25] have reported values of 2.08 and 2.55 eV for the electron-photodetachment threshold of $O_2^-$ in tetramethylsilane and 2,2,4-trimethylpentane, respectively.

The smaller the electron affinity of M becomes, the more the energy levels between $\pi_y$* and $\pi_M$* separate. Accordingly, the interaction energy $\epsilon_1$ decreases with EA of M. The smaller value of $\epsilon_1\epsilon_2/(\epsilon_2 - \epsilon_1)$ for FN than for MA is thus explicable. The decrease in $\epsilon_1\epsilon_2/(\epsilon_2 - \epsilon_1)$ in the order MA > MMA > DMMA is also attributable to the possible decrease in the electron affinity caused by methyl substitution; such a decrease occurs in methyl derivatives of benzoquinone.[20]

The optical bands of the complex anions are assignable to symmetry-allowed electron transitions from $(\pi_y^*)'$ to $(\pi_M^*)'$. The observed bands are structureless and broad, which are compatible with a transition due to intermolecular electron transfer. The increase in the observed band energy with decreasing electron affinity of M is also consistent with the electron-transfer band from $O_2^-$ to M. However, this band assignment necessarily requires that $\pi_M$* should lie more than 1 eV above $\pi_x$* of $O_2$. This requirement does not seem to be easily justified within the scope of simplified discussion connected with the electron affinity.

Shida reported that di-*tert*-butyl peroxide anions show a broad absorption band with a maximum at ca. 600 nm.[26] This band was ascribed to a transition from $\sigma$* of the O-O bond to $\sigma$* of the C-O bond.[26] The similarity of this band to the ones observed in the present study implies the possibility that the latter are also due to the same type of $\sigma$* transition of a peroxide anion in which two $\sigma$ bonds are formed between carbon atoms of the ethylene part of M and oxygen atoms. However, the anisotropy in $g$ value as found in the present ESR measurements has not been reported for the di-*tert*-butyl peroxide anion. It seems plausible that the substantial anisotropy does not appreciably occur in the case of $-O-O-^-$, since any conceivable excited state is too high to interact with the ground state. Even if the anisotropy occurred, the $g$ values estimated by eq 6 would be in the order of $g_x \simeq g_y > g_z \simeq 2.0023$. Consequently, the present optical bands do not seem to relate to the seemingly similar band of di-*tert*-butyl peroxide anions. So far, it is most reasonable to assign the optical absorption band to the electron transition from $O_2^-$ to M.

The energy level correlation postulated for $O_2^-\cdots M$ is applicable to the other complex anion, $O_2^-\cdots M_2$. The dimer anion referred to herein, such as $(MA)_2^-$ in reaction 1, is not an anion of $\sigma$-bonded dimer but is a complex stabilized by a charge resonance $MM^- \leftrightarrow M^-M$.[9,27] Thus, $M_2$ in the complex anion can be regarded as an associated molecule resulting from electron detachment from $M_2^-$. The orbital of $\pi_M$* splits when $M_2$ is formed, and the energy level of the SOMO for $M_2^-$ is lower than that for $M^-$. Then, the interaction of $M_2^-$ with $O_2$ may cause larger $\epsilon_1$ for complex ions $O_2^-\cdots M_2$ than that for $O_2^-\cdots M$, which is opposite to the observation for $\epsilon_1\epsilon_2/(\epsilon_2 - \epsilon_1)$ by ESR measurements. A possible explanation for this contradiction is that the split $\pi_M$* orbital in $O_2^-\cdots M_2$ interacts to less extent with $\pi_y$* than that in $O_2^-\cdots M$, because the former orbital must also interact with the other M to form the dimer $M_2$. If the optical band of $O_2^-\cdots M_2$ is assigned to a transition from $(\pi_y^*)'$ to the lower one of the split $(\pi_M^*)'$, the depression of $\pi_M$* accompanying the decrease in $\epsilon_1\epsilon_2/(\epsilon_2 - \epsilon_1)$ is consistent with the finding that the band energy for $O_2^-\cdots M_2$ is lower than that of the corresponding $O_2^-\cdots M$.

**Acknowledgment.** We are very grateful to Professors M. C. R. Symons and T. Shida for helpful discussions.

## References and Notes

(1) Bielski, B. H. J.; Richter, H. W. *J. Am. Chem. Soc.* **1977**, *99*, 3019.
(2) Eastland, G. W.; Symons, M. C. R. *J. Phys. Chem.* **1977**, *81*, 1502.
(3) Holroyd, R. A.; Bielski, B. H. J. *J. Am. Chem. Soc.* **1978**, *100*, 5796.
(4) Sawyer, D. T.; Giblan, M. J.; Morrison, M. M.; Seo, E. T. *J. Am. Chem. Soc.* **1978**, *100*, 627, and references cited therein.
(5) Valentine, J. S.; Curtis, A. B. *J. Am. Chem. Soc.* **1975**, *97*, 224.
(6) Bennett, J. E.; Ingram, D. J. E.; Symons, M. C. R.; George, P.; Griffith, J. S. *Philos. Mag.* **1955**, *46*, 443.
(7) Lunsford, J. H. *Catal. Rev.* **1973**, *8*, 135.
(8) Shida, T.; Iwata, S. *J. Am. Chem. Soc.* **1973**, *95*, 3473.
(9) Arai, S.; Kira, A.; Imamura, M. *J. Phys. Chem.* **1977**, *81*, 110.
(10) Kira, A.; Imamura, M. *J. Phys. Chem.* **1979**, *83*, 2267.
(11) Shida, T.; Iwata, S.; Imamura, M. *J. Phys. Chem.* **1974**, *78*, 741.
(12) Fukaya, M.; Muto, H.; Torlyama, K.; Iwasaki, M. *J. Phys. Chem.* **1976**, *80*, 728.
(13) Anbar, M.; Hart, E. J. "The Hydrated Electron"; Wiley-Interscience: New York, 1970.
(14) Che, M.; Tench, A. J.; Naccache, C. *J. Chem. Soc., Faraday Trans. 1* **1974**, *70*, 263.
(15) Che, M.; Tench, A. J. *Chem. Phys. Lett.* **1973**, *18*, 199.
(16) Morton, J. R.; Rowland, J. R.; Whiffen, P. H. *Natl. Phys. Lab. (U.K.), Bull.* **1962**, *BPR-13*.
(17) Kasai, P. H. *J. Chem. Phys.* **1965**, *43*, 3322.
(18) Carrington, A.; McLachlan, A. D. "Introduction to Magnetic Resonance"; Harper and Row: New York, 1967; Chapter 9.
(19) Younkin, J. M.; Smith, L. J.; Compton, R. N. *Theor. Chim. Acta* **1976**, *41*, 157.
(20) Chen, E. C. M.; Wentworth, W. E. *J. Chem. Phys.* **1975**, *63*, 3183.
(21) Peover, M. E. *Trans. Faraday Soc.* **1962**, *58*, 2370.
(22) Petrovich, J. P.; Baizer, M. M.; Ort, M. R. *J. Electrochem. Soc.* **1969**, *116*, 743.
(23) Kargin, Yu. M.; Kondranina, V. Z.; Kazakova, A. A.; Batyeva, E. S.; Samuilov, Ya. D. *Zh. Obshch. Khim.* **1974**, *46*, 741.
(24) Celotta, R.; Bannet, R.; Hale, J.; Siegel, M. W.; Levine, J. *Phys. Rev. A* **1972**, *6*, 631.
(25) Sowada, U.; Holroyd, R. A. *J. Chem. Phys.* **1979**, *70*, 3586.
(26) Shida, T. *J. Phys. Chem.* **1968**, *72*, 723.
(27) Ishitani, A.; Nagakura, S. *Mol. Phys.* **1967**, *12*, 1.